Size-segregated aerosol chemical composition at a boreal site in southern Finland, during the QUEST project

F. Cavalli, M. C. Facchini, S. Decesari, L. Emblico, M. Mircea, N. R. Jensen, S. Fuzzi

Atmos. Chem. Phys., 6, 993–1002, 2006
www.atmos-chem-phys.net/6/993/2006/

Atmospheric Chemistry and Physics

Size-segregated aerosol chemical composition at a boreal site in southern Finland, during the QUEST project

F. Cavalli[1], **M. C. Facchini**[1], **S. Decesari**[1], **L. Emblico**[1], **M. Mircea**[1], **N. R. Jensen**[2], **and S. Fuzzi**[1]

[1]Istituto di Scienze dell'Atmosfera e del Clima – CNR, Italy Via Gobetti 101, 40129 Bologna Italy
[2]European Commission, DG – Joint Research Centre, Institute of Environment and Sustainability, Climate Change Unit, 21020 Ispra, Italy

Received: 28 July 2005 – Published in Atmos. Chem. Phys. Discuss.: 16 September 2005
Revised: 20 December 2005 – Accepted: 3 January 2006 – Published: 28 March 2006

Abstract. Size-segregated aerosol samples were collected during the QUEST field campaign at Hyytiälä, a boreal forest site in Southern Finland, during spring 2003. Aerosol samples were selectively collected during both particle formation events and periods in which no particle formation occurred.

A comprehensive characterisation of the aerosol chemical properties (water-soluble inorganic and organic fraction) and an analysis of the relevant meteorological parameters revealed how aerosol chemistry and meteorology combine to determine a favorable "environment" for new particle formation. The results indicated that all *events*, typically favored during northerly air mass advection, were background aerosols (total mass concentrations range between 1.97 and 4.31 $\mu g\,m^{-3}$), with an increasingly pronounced marine character as the northerly air flow arrived progressively from the west and, in contrast, with a moderate SO_2-pollution influence as the air arrived from more easterly directions. Conversely, the *non-event* aerosol, transported from the south, exhibited the chemical features of European continental sites, with a marked increase in the concentrations of all major anthropogenic aerosol constituents. The higher *non-event* mass concentration (total mass concentrations range between 6.88 and 16.30 $\mu g\,m^{-3}$) and, thus, a larger surface area, tended to suppress new particle formation, more efficiently depleting potential gaseous precursors for nucleation. The analysis of water-soluble organic compounds showed that clean nucleation episodes were dominated by aliphatic biogenic species, while *non-events* were characterised by a large abundance of anthropogenic oxygenated species. Interestingly, a significant content of α-pinene photo-oxidation products was observed in the *events* aerosol, accounting for, on average, 72% of their WSOC; while only moderate amounts of these species were found in the *non-event* aerosol. If the organic vapors condensing onto accumulation mode particles are responsible also for the growth of newly formed thermodynamically stable clusters, our finding allows one to postulate that, at the site, α-pinene photo-oxidation products (and probably also photo-oxidation products from other terpenes) are the most likely species to contribute to the growth of nanometer-sized particles.

Correspondence to: F. Cavalli
(f.cavalli@isac.cnr.it)

1 Introduction

The formation of new aerosol particles in the atmosphere and their growth to CCN size have received considerable attention over recent years. Nucleation appears to be a frequent phenomenon in the continental boundary layer; and evidence of new particle formation has been reported for a variety of environments (Kulmala et al., 2004), including, for example, the Arctic and Antarctic regions (e.g. Wiedensohler et al., 1996), coastal areas of the North Atlantic (O'Dowd et al., 1998), the rural United Kingdom (Coe et al., 2002) and the industrialized agricultural regions of Germany and Italy (Birmili and Wiedensohler, 2000; Laaksoonen et al., 2005). Starting from 1996, aerosol formation and growth events have been observed also over the boreal forest of Finland (e.g. Mäkelä et al., 1997), typically occurring at daytime during cold Arctic and Polar air outbreaks (Nilsson et al., 2001). From previous measurements at the site, ternary nucleation (water-sulfuric acid-ammonia) has been hypothesized as the initial step in the particle formation mechanism (Kulmala et al., 2000), while low volatile photo-oxidation products from biogenic compounds emitted by trees have been postulated as being responsible for the subsequent growth, to observable sizes, of the particles in this environment (Kulmala et

Published by Copernicus GmbH on behalf of the European Geosciences Union.

al., 2003). Past experimental efforts have aimed to investigate the chemical composition of aerosol particles during nucleation episodes, and subsequently to compare it to that observed in no nucleation conditions (Mäekela et al., 2001). However, only small and rather inconclusive differences were detected, leaving unresolved questions on many chemical aspects of the phenomenon.

As part of the EC-project QUEST (Quantification of Aerosol Nucleation in the European Boundary Layer), the boreal forest of Finland has provided the focus for a new dedicated nucleation field experiment with the objective of refining our knowledge of the chemical and physical processes involved in the nucleation mechanism, and completing the picture of the conditions promoting particle formation.

In this study, we illustrate the size-dependent chemical composition of aerosol particles for nucleation and growth events and non-events, occurring during the intensive QUEST campaign, relating the chemical properties observed to the different origins and characters of the air masses advected to the measurement site. This analysis attempts to reveal the links between aerosol chemistry and meteorology in determining a favorable "environment" for atmospheric nucleation. In addition, the authors attempt to provide tentative indications as to the nature of the chemical species potentially involved in the growth of nucleated particles.

2 Experimental set up

Measurements were carried out at the SMEAR II station (Station for Measuring Forest Ecosystem-Atmosphere Relation) located at Hyytiälä, Southern Finland (61°51′ N, 24°17′ E, 181 m above sea level). The station represents a boreal coniferous forest dominated by Scots pine (*Pinus sylvestris* L.) with some Norway spruce (*Picea abies*) and birch (*Betula sp.*). A more detailed description of the site is given by Kulmala et al. (2001). The measurements were performed during the early spring (17 March–13 April) 2003. A special sampling strategy was designed to derive a complete size-segregated chemical characterisation of aerosol particles, during both particle formation events and periods in which no particle formation occurred. The aerosol samplers were employed, during daytime, some for the event sampling and some for the non-event sampling, driven by DMPS measurements. In Hyytiälä, nucleation events are generally expected during the late morning hours. In practise, if at that time nucleation mode particles appeared in the smallest DMPS channels, the event sampling started and generally lasted for the following hours in accordance with the persistence of new particle formation or growth of the nucleated mode. In contrast, if during the late morning no new particles were formed, the non-event sampling took place to the end of the day. Four "*event*" and four "*non-event*" samples were obtained during the one-month intensive campaign; each sample collected the *event* and *non-event days*, separately, occurring in the same week. The relatively long period of deployment of each sample was required in order to reach a sufficient aerosol load for reliable chemical analyses, especially in such remote forested areas. Thus, the sampling strategy adopted partially penalized the resolution in time in favor of a comprehensive chemical characterization.

Size-segregated aerosol samples were collected using Berner low-pressure impactors (flow rate 4.84 $m^3\,h^{-1}$), and particles were classified into five size fractions according to the following equivalent aerodynamic cut-off diameters at 50% efficiency: 0.05; 0.14; 0.42; 1.2; 3.5; 10 μm. In parallel, total aerosol samples were collected on quartz fiber filters using a high-volume sampler (flow rate 100 $m^3\,h^{-1}$).

Since the different analytical techniques employed are not compatible with any individual substrate, the impactor plate sampling substrate consisted of half a Tedlar foil on top of an aluminum foil; the combination of the two different sampling substrates allows for the derivation of a full description of the aerosol composition. On the (half) aluminum substrate, total aerosol mass was measured by weighing the substrate, before and after sampling, using a microbalance (Mettler Toledo MX/UMT2) in a controlled-environment chamber maintained at a temperature of 23±1°C and a relative humidity of 26±2%. A U ionizer was used to minimize weighing errors induced by electrostatic charge. The overall uncertainty of the aerosol mass concentration was calculated including (1) weighing precision, ±2 μg; (2) blank variability ±3.88 μg (n=8) and (3) uncertainty in the sampled air volume, ±3%.

On the (half) tedlar substrate, the whole water-soluble aerosol material was analysed. In particular, the concentration of inorganic ions was determined by ion chromatography and water-soluble organic carbon (WSOC) content by TOC liquid analyser. The random uncertainty for each aerosol component and each size range was computed using the procedure of error propagation described by Putaud et al. (2000). For correlated parameters, absolute uncertainties were conservatively added. The relative random uncertainties of the mean aerosol component concentrations for each impactor stage were obtained, including (1) uncertainty in the sampled air volume, ±3%; (2) precision of the extraction water volume, ±0.04 mL; (3) uncertainties in ion chromatography and WSOC measurements, ±5%; (4) uncertainties in the molecular mass to carbon ratios for carbonaceous species, and (5) blank variability, ±19.37, ±7.19, ±12.34, ±71.06, ±48.60, and ±124.64 $\mu g\,L^{-1}$ for Na^+, NH_4^+, Cl^-, NO_3^-, SO_4^{2-}, and WSOC, respectively.

In order to include the carbonaceous species in the aerosol mass budget, an average molecular mass to carbon mass ratio of 1.8, was adopted for WSOC, based on the speciation of WSOC performed on the samples (see Sect. 3.3).

Quartz filters were entirely devoted to the characterisation of the water-soluble organic compounds by adopting the procedure proposed by Decesari et al. (2000). Employing

this procedure, the WSOC mixture was separated by ion exchange chromatography into three main classes of compounds: a) neutral compounds; b) mono- and di-carboxylic acids; c) polycarboxylic acids, and a functional group analysis was performed by Proton Nuclear Magnetic Resonance (H-NMR).

3 Results and discussion

3.1 Overview of meteorology and new particle formation activity during the intensive campaign

The air mass analysis was performed using back-trajectories which were calculated, throughout the experiment, using a long-range transport model SILAM (Sofiev and Siljamo, 2003), maintained by the Finnish Meteorological Institute. The air parcel back-trajectories arriving at Hyytiälä on the 925 hPa pressure levels were calculated typically 96 h backwards in time in 6 h intervals. Furthermore, meteorological parameters (wind direction, global radiation, precipitation indicator) and trace gases, continuously monitored at the station, were evaluated during the periods of activated *event* and *non-event* sampling. The prevailing wind directions, calculated as a percentage of total time by sector at the field station above the tree-top level (16.8 m), are displayed in Fig. 1. Although the period of deployment of each sample was relatively long (i.e. seven days), the wind roses in Fig. 1 show that the conditions experienced during the individual *event* and *non-event* samples were relatively homogenous and each sample could be reasonably associated to a definite major prevailing wind sector.

The intensive field campaign was characterized by a high number of days with a detectable new particle formation, and only a few days with no significant nucleation activity. Among the particle formation days, a further differentiation could be made between days on which the nucleation mode was easily distinguishable until it had grown to the Aitken size mode, and days on which the particle growth was less distinct or not sufficiently long. In agreement with previous observations (Nilsson et al., 2001) at this site, the prevailing wind sector and air trajectory analyses indicated that new particle formation events were typically favored during northerly advection. In particular, nucleation events appeared to be more frequent and intense in air masses from the north-to-west sector (*e*170303–230303 and *e*240303–300303). Such air masses, of a primarily Arctic/Polar origin, had traveled over the ocean and briefly over Scandinavian regions before reaching the measurement station. The advection of Arctic/Polar air masses from more easterly directions, i.e. after passing over parts of northwest Russia, (*e*070403–130403) seemed, instead, to weaken slightly the nucleation activity. In contrast, southern transport including important advection over either Northern Great Britain and Denmark (*ne*170303–230303 and *ne*240303–300303) or

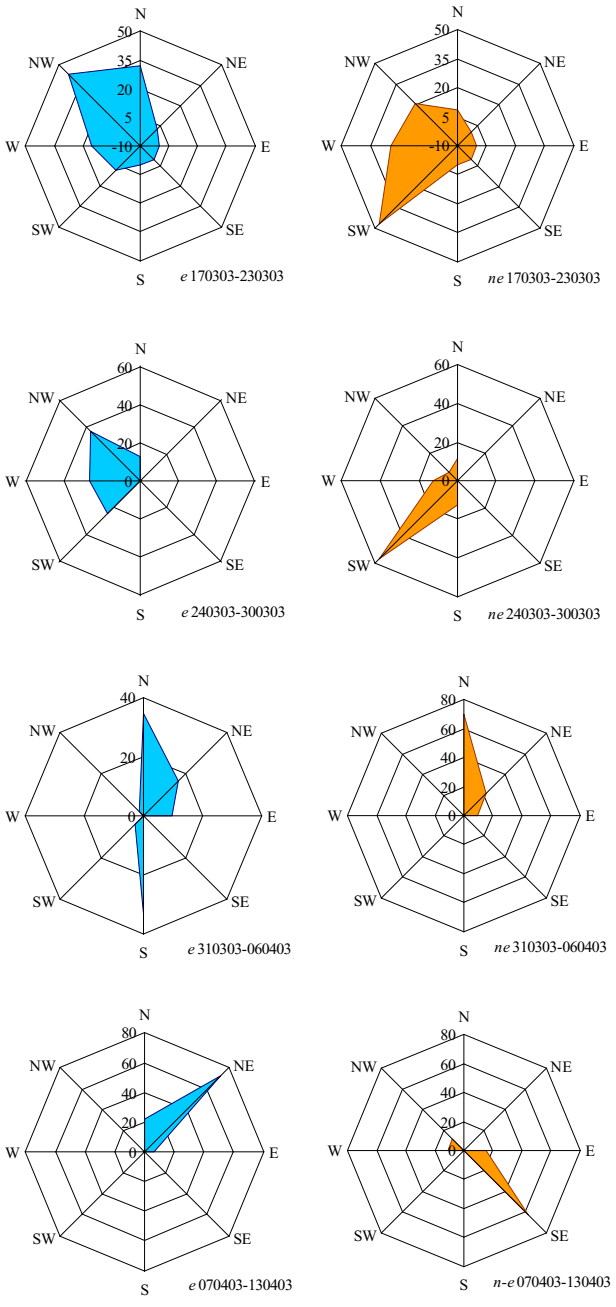

Fig. 1. Prevailing wind sectors calculated as a percentage of total time by sector at the field station above the tree-top level (16.8 m) during the activated *event* and *non-event* sampling periods.

over the east-central European latitudes (*ne*07403–130403) tended to prevent new particle formation (Fig. 1). The week 31 March–6 April 2003, only apparently, represents an exception to this tendency. A careful analysis of the backward trajectories arriving at Hyytiälä during this week clarified the puzzling southerly wind directions detected for the *event* sample and the northerly ones for the *non-event* sample. The entire week was dominated by air mass advection

from the Arctic/Polar region: in particular, during some *event* days, the northerly air masses slightly bypassed the measurement site and reached it later from a southerly direction; conversely, during the only *non-event* day, the trajectories evolved progressively in larger loops and finally came in from the north.

3.2 Mass concentration and size-segregated chemical composition

Table 1 reports the total aerosol mass concentrations obtained by adding the gravimetric-measured mass of the five impactor stages; the corresponding submicron (Dae$<$1.2 μm) and supermicron (Dae$>$1.2 μm) values for all aerosol samples are also indicated. The total mass concentrations for all *event* samples are extremely low, ranging between 1.97 and 4.31 $\mu g\,m^{-3}$. The submicron concentration shows rather similar values for the three *events* -*e*170303–230303, *e*240303–300303 and *e*310303–060403 – when advection occurred mainly within the north-to-west sector, on average 1.40$\pm$0.14 $\mu g\,m^{-3}$; while a higher value is found for *e*070403–130403 when air flows from the northeast may have transported polluted air from the Kola Peninsula, in Russia to the measurement site (Ruuskanen et al., 2003). A particularly pronounced supermicron mode is measured for *e*240303–300303, indicating the prevalently maritime nature of the aerosol. The total mass concentrations for the *non-event* samples are shifted towards relatively higher values, between 6.88 and 16.30 $\mu g\,m^{-3}$, the highest submicron mass concentrations being observed when the air masses arrive from southwest directions. In general, all *non-event* samples exhibit, compared to the corresponding *event* samples of the same week, a more pronounced submicron mode, while a significant increase in the supermicron mode is limited to southwesterly air masses. Only a small difference is observed between the total mass concentration of *ne*310303–060403, 4.08$\pm$0.29, and that of the corresponding *event*, 2.51$\pm$0.16: the *ne*310303–060403 collects, however, the only *non-event* day occurred in that week. On this day, despite the favorable Arctic/Polar air masses and the limited pre-existing aerosol load, low values of global radiation and precipitation prevented aerosol formation through the reduced photochemistry and wet scavenging of precursor gases.

After a combined evaluation, on a weekly basis, of the meteorological parameters, trajectories, nucleation activity, and chemical compositions, two *events* and corresponding *non-events* were selected as significant case studies: *e*240303–300303, *ne*240303–300303 and *e*070403–130403, *ne*070403–130403. Referring each to air mass advection from a different 90°-wind sector, the four selected samples together provide a good overview of the various conditions encountered during the campaign (Fig. 1).

Figure 2 shows the size-segregated aerosol composition for the four selected samples. The height of each bar represents the gravimetrically measured mass. The component labelled 'unaccounted' is the difference between the weighed mass and the sum of analysed aerosol chemical components. Figure 2 also illustrates the percentage contribution of the aerosol constituents to the submicron aerosol mass.

The size-distributions and concentrations of the analysed species for *e*240303–300303 are typical of a marine aerosol following the north-westerly flow, bringing a maritime Arctic/Polar air mass to the sampling station. Na^+ together with the other sea-salt ions, Cl^-, Mg^{2+}, Ca^{2+} and K^+, are associated in a pronounced mode at supermicron size; the NO_3^- contributes 0.18$\pm$0.01 $\mu g\,m^{-3}$ to the supermicron mode, partitioning itself in favor of the more alkaline coarse particles, as it typically occurs in marine aerosol. The nss-SO_4^{2-} submicron concentration of 0.27$\pm$0.01 $\mu g\,m^{-3}$ is in agreement with previous observations in forested sites under the influence of clean marine air masses after a passage of a frontal system (Kavouras et al., 1998; Shantz et al., 2004). The bulk WSOC concentration is 0.42$\pm$0.04 $\mu g\,m^{-3}$. Both nss-SO_4^{2-} and WSOC concentrations are comparable to the values recently observed in clean marine aerosol over the North Atlantic (Cavalli et al., 2004), supporting the background marine nature of this *event* aerosol. During the same week, *non-event* aerosol carried much of its original maritime character, following the persistent advection of mainly westerly air masses. However, advection over Northern Great Britain and Denmark (southerly components) results in a clear change of chemical characteristics. The *non-event* submicron mass concentrations of nss-SO_4^{2-}, NH_4^+ and WSOC are now significantly larger, amounting to 2.32$\pm$0.12 $\mu g\,m^{-3,}$, 2.07$\pm$0.10 $\mu g\,m^{-3}$ and 1.78$\pm$0.12 $\mu g\,m^{-3}$, respectively. NO_3^- shows a broader size distribution with a total mass concentration of 4.10$\pm$0.16 $\mu g\,m^{-3}$, the highest one measured during the experiment. NO_3^- is, therefore, the main individual component, contributing 26% to the total aerosol mass. Similarly, during the 7–13 April 2003 week, two well-distinguished situations (*event* and *non-event* samples) are found. The *e*070403–130403 offers an example of air masses from the northeast, with aerosol having a slightly modified Polar behavior. The supermicron mode comprises sea-salt and the associated NO_3^- with a supermicron mass concentration of 0.12$\pm$0.01 $\mu g\,m^{-3}$, confirming the maritime polar nature of the aerosol. In contrast, the submicron mode is mainly composed of nss-SO_4^{2-} with a relatively high mass concentration of 1.11$\pm$0.05 $\mu g\,m^{-3}$, in accordance with the route over the polluted Kola Peninsula and northwest Russia. The remaining species, NH_4^+ and WSOC, contribute 0.21$\pm$0.01 $\mu g\,m^{-3}$ and 0.425$\pm$0.05 $\mu g\,m^{-3}$, respectively to the submicron mode.

In the same week, the *non-event* days occurred when air masses, originating over the east-central European latitudes, reached the measuring site coming from an east to south-east direction. The change in the air mass origin is clearly

Table 1. Total aerosol mass concentrations, in $\mu g\,m^{-3}$ units, and the corresponding submicron and supermicron values (obtained by adding the gravimetric-measured mass of the impactor stages) for all *event* and *non-event* aerosol samples.

	Sampling time (h)	Total	Submicron	Supermicron
event				
*e*170303–230303	17	1.97±0.25	1.26±0.20	0.71±0.16
*e*240303–300303	35	3.60±0.14	1.40±0.10	2.20±0.09
*e*310303–060403	27	2.51±0.16	1.54±0.13	0.97±0.10
*e*070403–130403	23	4.31±0.20	3.5±0.16	0.81±0.11
non-event				
*ne*170303–230303	26	6.88±0.22	3.57±0.16	3.31±0.14
*ne*240303–300303	18	16.30±0.38	9.12±0.30	7.17±0.24
*ne*310303–060403	16	4.08±0.29	2.56±0.22	1.52±0.18
*ne*070403–130403	30	7.78±0.21	6.81±0.19	0.97±0.10

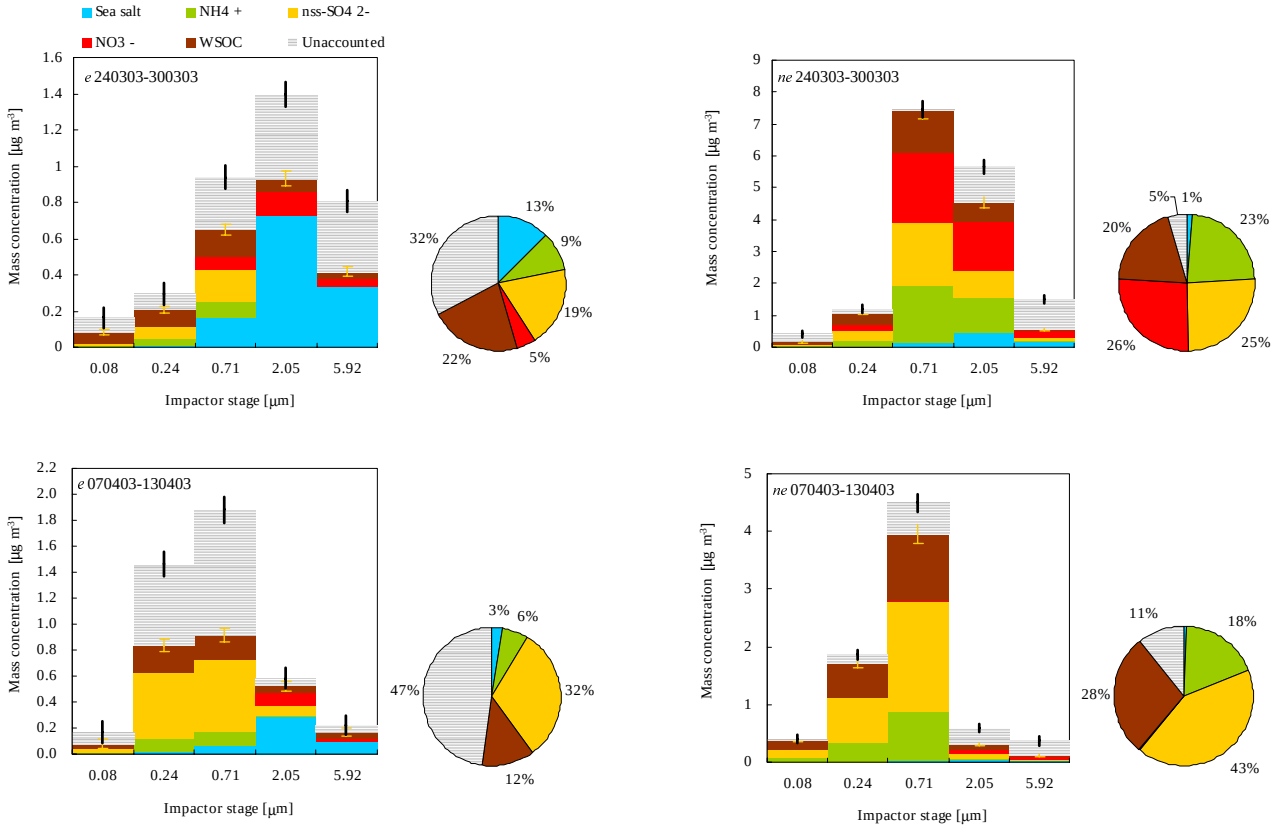

Fig. 2. Size-segregated aerosol composition for four selected samples (*e*240303–300303, *ne*240303–300303 and *e*070403, *n*−*e*070403). "Unaccounted" is the difference between the total weighed mass and the total analysed mass. Black bars represent the overall uncertainties associated with the weighed mass, and yellow bars represent the overall uncertainties of the total analysed mass. The percentage contribution of the aerosol constituents to the submicron aerosol mass is also shown.

reflected by the variation in the aerosol chemical properties, and, especially, in the increase of the submicron concentration of the anthropogenic nss-SO_4^{2-}, 2.58±0.12 $\mu g\,m^{-3}$, alone accounting for 42% of the total submicron mass. The $NH4^+$ and WSOC also contribute to the submicron mode with concentrations of 1.24±0.05 $\mu g\,m^{-3}$ and 1.19±0.11 $\mu g\,m^{-3}$, respectively. Interestingly, no major changes occurred over the entire size range in the mass concentration of NO_3^- which remained at the low level of 0.11±0.1 $\mu g\,m^{-3}$.

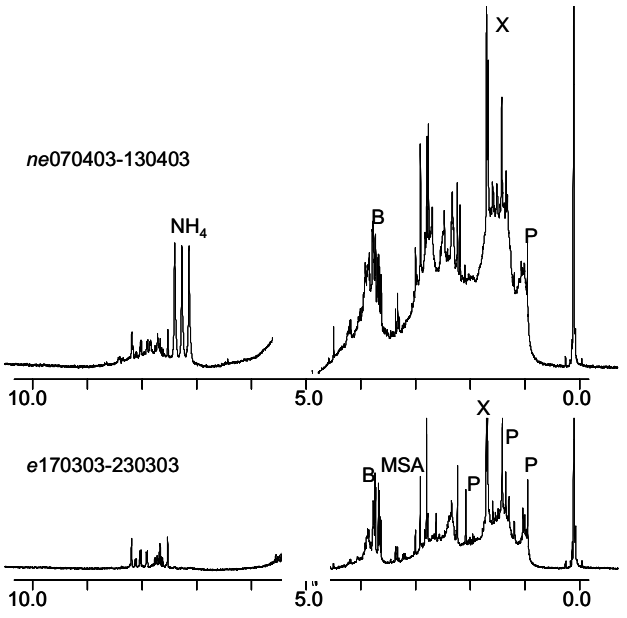

Fig. 3. H-NMR spectra of two the aerosol samples, *e*170303–230303 and *ne*07403–130403. X is an unidentified compounds, possibly biogenic, responsible for the peaks at 1.57–1.59 ppm; P is pinonic acid and B is a contaminant from the sampling/analytical procedure.

As shown in Fig. 2, the "unaccounted" category represents a significant fraction of the submicron aerosol for both *e*240303–300303 and *e*070403–130403 *events*, whereas its contribution drops considerably for the corresponding *non-event*s. Aerosol species not determined in this study, such as water-insoluble carbon, black carbon and soil-derived insoluble material can account for the mass discrepancy observed. Water-insoluble species appear, therefore, to contribute more significantly to the *event* aerosol.

The experimental evidence clearly indicates that new particle formation is preferentially connected to the clean conditions of northerly Arctic/Polar air masses: all *events* are background aerosols, with a marine character (Na^+ content in the coarse particles) that becomes more pronounced as the northerly air flow arrives from more westerly directions and, in contrast, with a moderate SO_2-pollution influence as the air arrives from more easterly directions. The *non-event* aerosol loses the natural character exhibited by the *event* one and acquires, instead, chemical features resembling those of European continental sites, with a marked increase in concentration of all major anthropogenic aerosol constituents. The chemical data, both trace gases and aerosol species concentrations, reflect distinct source strengths for the two *non-events* described above. One, *ne*240303–300303, shows pollution features typical of the western central European countries where the high traffic density accounts for stronger NO_x emissions and, consequently, higher concentrations of NO_3^- which comprises the most abundant total aerosol mass fraction. The other, *ne*070403–130403, is typical of eastern European regions where, as a consequence of domestic coal heating and coal-fired power plant emissions, the gaseous levels of $SO_2$are at high values, 0.7 ppb, and the nss-SO_4^{2-} represents the main individual submicron aerosol component.

In general, the *non-event* aerosol chemical characteristics can explain the suppression of new particle formation: the higher mass concentrations and, thus, the larger surface area of the pre-existing *non-event* aerosols, act as a more effective condensational sink depleting the potential gaseous precursors for new particle production.

3.3 Water-soluble organic compound analysis

Analysis of organic functional groups was performed by H-NMR on the total aerosol samples, for *events* and *non-events*, collected during the campaign. The H-NMR spectra are characterised by several sharp resonances from individual compounds superimposed on a strong background signal from unresolved complex mixtures of substances. The background signals are distributed among a few main broad bands, which can be attributed to the following categories of functional groups on the basis of the intervals of chemical shift (δ_H): alkylic moieties (H-C, δ_H: 0.9–1.9 ppm); aliphatic CH groups bound to an unsaturated carbon (H-C-C=, δ_H: 1.9–3.2 ppm); hydroxyl groups and ethers (H-C-O, δ_H: 3.2–4.2 ppm), aromatic rings (H-Ar, 6.5–8.5 ppm). Weak broad signals from aldehydes (H-C=O) are occasionally observed between 9.5 and 10.5 ppm. Although they account, on average, for less than 1% of the total integral of the spectra, their occurrence is remarkable, as they were never observed in atmospheric aerosol samples under H-NMR analysis (Decesari et al., 2000; Decesari et al., 2001; McFiggans et al., 2006[1]).

Figure 3 reports as an example the H-NMR spectra of two aerosol samples, one *event* and one *non-event* sample, with significantly different air mass history.

Sharp resonances are very prominent in the spectrum of *e*170303–240303, collected under the clean air mass advections from N-NW sectors, which does not resemble any other of the H-NMR spectra have collected so far (Decesari et al., 2000; Decesari et al., 2001; McFiggans et al., 2006[1]). The intense singlets at 0.85, 1.32 and 2.13 ppm of chemical shift and some less intense multiplets in the *e*170303–240303 spectrum are attributed to pinonic acid on the basis of a comparison with the spectrum of the pure compound. Weaker signals from pinic acid at 0.94 ppm are also identified. Pinonic acid and pinic acid are only a fraction of the low volatile photo-oxidation products of α-pinene detected

[1]McFiggans, G., Topping, D. O., Cubison, M. J., Allan, J. D., Coe, H., Bower, K. N., Emblico, L., Decesari, S., Facchini, M. C.: Aerosol composition – hygroscopicity closure using ADDEM, a multicomponent thermodynamic model including the effects of curvature, to be submitted to Atmos. Chem. Phys. Discuss., 2006.

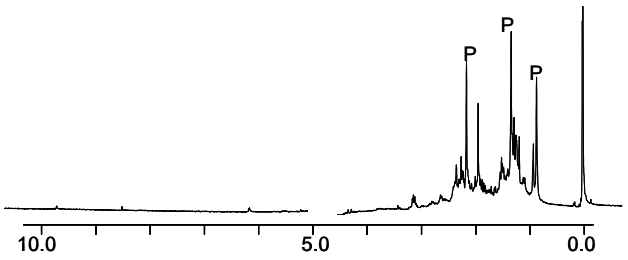

Fig. 4. H-NMR spectrum of secondary organic aerosols generated from the photo-oxidation of α-pinene, in smog chamber experiments. P is pinonic acid.

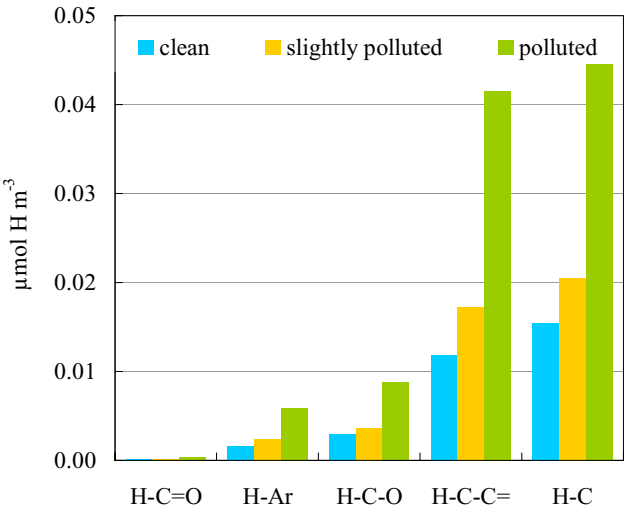

Fig. 5. Average concentration (μmol H m^{-3} units) of the main function group categories described in the text for the three cases, clean, slightly polluted and polluted.

in the particle phase (Kavouras et al., 1998, and references therein). As confirmation, Fig. 4 reports the H-NMR spectrum of secondary organic aerosols (SOA) generated from the photo-oxidation of α-pinene, in smog chamber experiments. The experiments were performed in a 480 L reaction chamber, equipped with on-line FT-IR (Fourier Transformed Infrared Spectroscopy) and a DMA (differential mobility analyzer) to follow the reaction [5 to 10 ppmV of α-pinene was mixed with 5 to 11 ppmV of methyl nitrite, CH_3ONO, and 2.5 to 5 ppmV of NO. Then UV-light was switched on ($\lambda \geq 300$ nm) to produce OH radicals and thereby initiate the photo-oxidation of α-pinene and the production of organic aerosols were observed. These aerosols were then collected on Teflon filters (Teflon filter without support, type=LS, "pore size=5 μm", diameter=47 mm, the filters were washed with Milli-Q water and dried in a clean chamber before use, calculated volume from the DMA$\sim$150 μg). The filters were then stored below 5 degree Celsius before analysis. For more details about the set-up and handling of the reaction chamber see Ballesteros et al., 2002].

A comparison between the two spectra reveals that α-pinene oxidation products may account for most of the spectral features of the *event* aerosol observed between 0.9 and 2.3 ppm of chemical shift, with respect to both sharp resonances and background signals. A strong resonance, absent in the laboratory-generated SOA spectrum, arises from two overlapping peaks at 1.57 and 1.59 ppm of chemical shift. Its occurrence at high intensity particularly under clean northerly flows allows the attribution of the signal to an unidentified biogenic compound present in concentrations comparable to that of pinonic acid, or even higher. Other terpenes, such as Δ^3-carene, β-pinene and camphene, are, in fact, known to be emitted in a conifer forested atmosphere (Spanke et al., 2001). It is, therefore, conceivable that biogenic compounds account for a significant portion of aerosol WSOC in the sample in question.

Furthermore, a minor fraction of the background signals in *e*170303–230303, especially those resulting from aromatic and more oxidised groups – which cannot be reconciled with the composition of α-pinene photo-oxidation products – may be due to anthropogenic compounds from local pollution sources.

The background signal is, in contrast, dominant in the spectrum of *ne*070403–130403, collected under south easterly polluted flows, which exhibits a marked similarity to those of water soluble organic compounds from European continental environments (Decesari et al., 2001; McFiggans et al., 2006[1]). Peaks at 0.85 and at 1.57–1.59 ppm indicate, however, that biogenic species, although in relatively low concentrations, are found also under anthropogencally polluted conditions.

In general, on the basis of the H-NMR spectra patterns, the collected samples could be classified into three cases (Table 2): a "clean case" when biogenic/natural sharp signals (e.g. Fig. 3, *e*170303–230303) dominate the spectrum; a "polluted case" when broad anthropogenic pollution features (e.g. Fig. 3, *ne*070403–130403) prevail and, finally, an intermediate, slightly polluted case when the two components are equally combined. As shown in Table 2, the analysis on WSOC composition further corroborates the evidence that clean conditions result to be mainly associated to nucleation events (i.e. *e*170303–240303, *e*240303–300303, *e*310303–060403 and *ne*310303–060403. Note that for *ne*310303–060403, reduced photochemistry and wet-scavenging suppressed particle formation), while polluted conditions prevent them (i.e. *ne*240303–300303 and *ne*07403–130403). Under low pollution levels, other factors, like precipitation and cloudiness, appear to be crucial in determining the formation of new aerosol particles (i.e. *ne*170303–230303 and *e*07403–130403).

In Table 2, the three cases are quantitatively described in terms of the total mass concentrations (from impactor data), average WSOC concentrations (filter data), μmol/m^3 of non-exchangeable organic H determined as the total integrals of

Table 2. Total mass concentrations (from impactor data), average WSOC concentrations (filter data), μmol/m^3 of non-exchangeable organic H determined as the total integrals of the H-NMR spectra, and functional group composition for the three cases, clean, slightly polluted and polluted.

Case	Samples	Total mass conc. [μg/m^3]	WSOC [μg/m^3]	μmol H/m^3	Functional group composition [% of total μmol H]							
					H-C=O	H-Ar	H-C-O	H-C-C=				H-C
								3.2–3.4	2.5–3.2	1.9–2.5	MSA	individual peaks	individual peaks
Clean	*e*170303-230303 *e*240303–300303 *e*310303–060403 *ne*310303–060403	2 to 4	0.360	0.031	0.4% (0.2%)	5.2% (0.7%)	9.2% (2.0%)	1.6% (0.4%)	15.8% (1.8%)	20.0% (0.5%)	0.7% (0.4%)	2.4% (0.7%)	48.7% (0.5%) 7.6% (1.0%)
Slightly polluted	*ne*170303–230303 *e*070403–130403	4 to 7	0.482	0.044	0.2% (0.1%)	5.5% (0.4%)	8.4% (0.9%)	1.6% (0.1%)	18.2% (1.3%)	19.8% (1.3%)	0.6% (0.2%)	2.7% (0.4%)	46.9% (1.9%) 6.0% (2.3%)
Polluted	*ne*240303–300303 *ne*070403–130403	>7	1.676	0.100	0.4%	5.9% (1.5%)	8.7% (3.0%)	1.3% (0.5%)	20.0% (2.6%)	19.9% (0.5%)	0.3% (0.2%)	1.4% (0.1%)	44.3% (1.5%) 3.8% (0.6%)

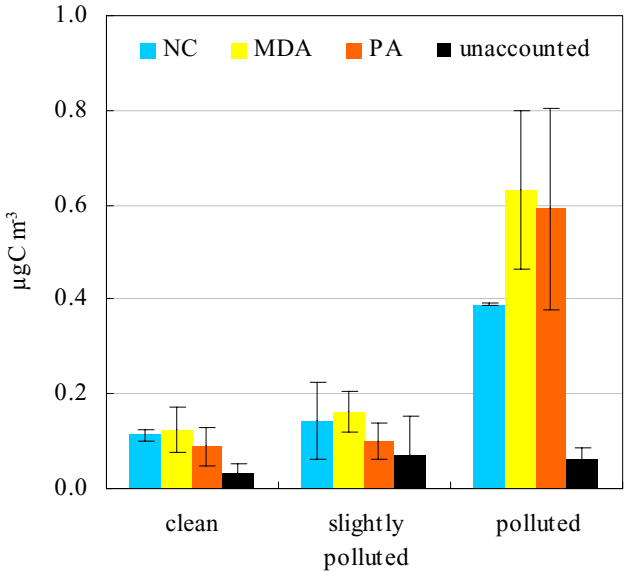

Fig. 6. Average concentrations (μgC m^{-3} units) of neutral compounds NC, mono- and di-carboxylic acids MDA, policarboxylic acids PA, and unrecovered WSOC for the three cases, clean, slightly polluted and polluted.

the H-NMR spectra, and H-NMR compositions (see also Fig. 5). Differences in background signals are mainly observed with respect to the complex structure of bands in the interval 1.8–3.4 ppm, arising from aliphatic groups bound to an unsaturated carbon (H-C-C=). The percentage concentrations of those hydrogen atoms are provided for three sub-ranges of chemical shift: 1.8–2.5, 2.5–3.2, and 3.2–3.4 ppm. The higher content of H-C-C= groups in the chemical shift interval of 2.5–3.2 ppm in polluted cases as compared to clean ones, indicate the larger amount of fairly oxidised structures, containing unsaturated carbon atoms separated by very short aliphatic chains, such as in succinic acid ($\delta_H \sim 2.65$) in polluted air masses. In contrast, a larger abundance of aliphatic structures, H-C, characterises the cleaner cases, together with a higher content of hydrogen atoms detected as individual peaks from biogenic species, as α-pinene photo-oxidation products, MSA and other biogenic species (see supplementary material).

If we assume that the laboratory percentage yields of the individual aerosol products from α-pinene photo-oxidation (Fig. 4) remain unchanged in ambient air conditions, the overall contribution of α-pinene photo-oxidation products to the WSOC in the Hyytiälä samples can be estimated by normalising the various H-NMR signals to that of the methylic hydrogen atoms of pinonic acid at 0.85 ppm. The resulting organic fraction attributable to oxidation products of α-pinene spans from 72% in samples collected under clean (*events*) and moderately polluted conditions, down to 32% in samples of aerosol in more polluted air masses (*non-event*).

Another insight into the composition of Hyytiala WSOC is provided by the fractionation of the sample water extracts into neutral compounds (NC), mono/di-acids (MDA) and polyacids (PA) (see Sect. 2). Figure 6 shows the average concentrations of NC, MDA, PA and unrecovered WSOC for the three cases, clean, slightly polluted and polluted. The concentrations of three broad classes of WSOC are generally correlated with those of total water-soluble carbon, revealing higher values during the most polluted conditions. Water-soluble organic carbon, not accounted for by HPLC analysis (i.e. unrecovered WSOC) ranges from 4% to 17%, on average. Mono/di-acids are the most abundant class of WSOC in all cases. Neutral compounds appeared to be almost as concentrated as MDA when the air masses advected to the site were clean or only slightly polluted (33%); under these conditions, polyacids (PA) account for 21–24% of WSOC. This percentage increased up to 35% in the more polluted cases, whereas the contribution of NC decreased to 24%. The high relative concentrations of PA and the low contribution of NC encountered when air masses transported to the site pollution from Central Europe are characteristic of anthropogenic WSOC from fossil fuel combustion, with little contribution from biomass burning (Decesari et al., 2001). Conversely,

aerosol WSOC in pristine air masses exhibits low PA concentrations associated with a relatively high contribution of NC and MDA (Cavalli et al., 2004).

4 Conclusions

Size-dependent chemical composition of aerosol particles for nucleation and growth events and non-events, occurring during the intensive QUEST campaign at Hyytiälä, Southern Finland, highlighted the links between air masses, chemistry and new aerosol particle formation.

Prevailing wind sector and air trajectory analyses, limited to the activated sampling periods, indicate that new particle formation events are typically favored during northerly air mass advection, more markedly so when it occurs from the north-to-west sector than from the north-to-east one, while new particles never form in air masses from southerly directions. The data obtained on the chemical composition show that all *events* are background aerosols (total mass concentrations range between 1.97 and 4.31 $\mu g\,m^{-3}$) with an increasingly marine character (Na^+ content in the coarse particles) as the northerly air flow are progressively from the west and, in contrast, with a moderate SO_2-pollution influence as the air arrives from more easterly directions. The *non-event* aerosol loses the natural character and acquires, instead, chemical features resembling those of European continental sites, with a marked increase in the concentrations of all major anthropogenic aerosol constituents. The analysis on WSOC composition further corroborates the evidence that clean conditions, dominated by aliphatic biogenic species, favour nucleation episodes, while polluted conditions with a large abundance of anthropogenic oxygenated species prevent them. Under low pollution levels, other factors, like precipitation and cloudiness, appear to be crucial in regulating the formation of new aerosol particles. In general, the *non-event* aerosol characteristics can well account for the suppression of new particle formation; the higher mass concentrations and, thus, a larger surface area of the pre-existing *non-event* aerosols, act as a more effective condensational sink depleting the potential gaseous precursors for new particle production. The large variations in the aerosol chemical composition found between *events* and *non-event* episodes reveal how meteorological and chemical factors combine to determine the favorable "environment" for atmospheric nucleation of new aerosol particles. Further efforts should now be made to understand whether, as well as mass concentration, the chemical composition of pre-existing aerosol may also constitute a limiting factor for particle formation.

Furthermore, a large abundance of α-pinene photo-oxidation products has been observed in the *events* aerosol, accounting for, on average, 72% of their WSOC content; while only moderate amounts of these products are found in the *non-event* aerosol. The AMS measurements (Allan et al., 2006) performed during nucleation episodes, reveal the same organic signature in the nucleation/Aitken mode and in the accumulation mode, implying that the organic vapors responsible for the growth of newly formed clusters condense also onto particles of larger diameter. This finding allows one to postulate that, α-pinene photo-oxidation products (and probably also photo-oxidation products from other terpenes) are the most likely species to contribute to the growth of nanometer-sized particles at this site.

Acknowledgements. The authors would like to thank J. Paatero from Finnish Meteorological Institute for generating air mass back trajectory maps, and P. Aalto and the personnel of the SMEAR II station for providing DMPS, meteorological and gas data. R. Manca and L. Marelli from DG-JRC are gratefully acknowledged for the help with the α-pinene experiments in the laboratory. The work was supported by the European Commission under contract EVK2-CT2001-00127 (QUEST) and EVK2-CT-2001-00098 (PHOENICS).

Edited by: A. Laaksonen

References

Allan, J. D., Alfarra, M. R., Bower, N. K., Coe, H., Jayne, J. T., Worsnop, D. R., Aalto, P. P., Kulmala, M., Hyötyläinen, T., Cavalli, F., and Laaksonen, A.: Size and composition measurements of background aerosol and new particle growth in a Finnish forest during QUEST 2 using an Aerodyne Aerosol Mass Spectrometer, Atmos. Chem. Phys., 6, 315–327, 2006.

Ballesteros, B., Jensen, N. R., and Hjorth, J.: FT-IR study of the kinetics and products of the reactions of dimethylsulphide, dimethylsulfoxide and dimethylsulphone with Br and BrO, J. Atmos. Chem., 43, 135–150, 2002.

Birmili, W. and Wiedensohler, A.: New particle formation in the continental boundary layer: Meteorological and gas phase parameter influence, Geophys. Res. Lett., 27, 3325–3328, 2000.

Cavalli, F., Facchini, M.C., Decesari, S., Mircea, M., Emblico, L., Fuzzi, S., Ceburnis, D., Yoon, Y. J., O'Dowd, C. D., Putaud, J.-P., and Dell'Acqua, A.: Advances in characterisation of size resolved organic matter in marine aerosol over the North Atlantic, J. Geophys. Res., 109, doi:10.1029/2004JD0051377, 2004.

Coe, H., Williams, P. I., McFiggans, G., Gallagher, M. W., Beswick, K. M., Bower, K. N., and Choularton, T. W.: Behaviour of ultrafine particles in continental and marine air masses at a a rural site in the United Kingdom, J. Geophys. Res., 105, 26 581–26 905, 2002.

Decesari, S., Facchini, M. C., Fuzzi, S., and Tagliavini, E.: Characterization of water-soluble organic compounds in atmospheric aerosol: A new approach, J. Geophys. Res., 105, 1481–1489, 2000.

Decesari, S., Facchini, M. C., Matta, E., Lettini, F., Mircea, M., Fuzzi, S., Tagliavini, E., and Putaud, J.-P.: Chemical features and seasonal variation of the fine aerosol water-soluble organic compounds in the Po Valley, Italy, Atmos. Environ., 35, 3691–3699, 2001.

Kavouras, I. G., Mihalopoulos, N., and Stephanou, E. G.: Formation of atmospheric particles from organic acids produced by forests, Nature, 395, 683–686, 1998.

Kulmala, M., Pirjola, U., and Mäkelä, J. M.: Stable sulphate clusters as a source of new atmospheric particles, Nature, 404, 66–69, 2000.

Kulmala, M., Hameri, K., Aalto, P. P., Makela, J. M., Pirjola, L., Nilsson, E. D., Buzorius, G., Rannik, U., Maso, M., Seidl, W., Hoffman, T., Janson, R., Hansson, H.-C., Viisanen, Y., Laaksonen, A., and O'Dowd, C.: Overview of the international project on biogenic aerosol formation in the Boreal forest (BIOFOR), Tellus 53B, 324–343, 2001.

Kulmala, M., Suni, T., Lehtinen1, K. E. J., Dal Maso, M., Boy, M., Reissell, A., Rannik, U., Aalto, P., Keronen, P., Hakola, H., Bäck, J., Hoffmann, T., Vesala T., and Hari, P.: A new feedback mechanism linking forests, aerosols, and climate, Atmos. Chem. Phys., 4, 557–562, 2004,
SRef-ID: 1680-7324/acp/2004-4-557.

Kulmala, M., Vehkamäki, H., Petäjä, T., Dal Maso, M., Lauri, A., Kerminen, V.-M., Birmili, W., and McMurry, P. H.: Formation and growth rates of ultrafine atmospheric particles: A review of observations, J. Aerosol Sci., 35, 143–176, 2004.

Laaksonen, A., Hamed, A., Joutsensaari, J., Hiltunen, L., Cavalli, F., Junkermann, W., Asmi, A., Fuzzi, S., and Facchini, M. C.: Cloud condensation nucleus production from nucleation events at a highly polluted region, Geophys. Res. Lett, 32, L06812, doi:10.1029/2004GL022092, 2005.

Mäkelä, J. M., Aalto, P., Jokinen, V., Nissinen, A., Palmroth, S., Markkanen, T., Seitsonen, K., Lihavainen, H., and Kulmala, M.: Observation of ultrafine aerosol particle formation and growth in boreal forest, Geophys. Res. Lett, 24, 1219–1222, 1997.

Mäkelä, J. M., Yli-Koivisto, S., Hiltunen, V., Seidl, W., Swietlicki, E., Teinilä, K., Sillanpää, M., Koponen, I. K., Paatero, J., and Rosman, K.: Chemical composition of aerosol during particle formation events in boreal forest, Tellus 53B, 380–393, 2001.

Nilsson, E. D., Paatero, J., and Boy, M.: Effect of air masses and synoptic weather on aerosol formation in the continental boundary layer, Tellus, 53B, 462–478, 2001.

O'Dowd, C. D., Geever, M., Hill, M. K., Jennings, S. K., and Smith, M. K.: New particle formation and spatial scale in the clean marine coastal environment, Geophys. Res. Lett., 25, 1661–1664, 1998.

Putaud, J-P., Van Dingenen, R., Mangoni, M., Virkkula, A., Raes, F., Maring, H., Prospero, J. M., Swietlicki, E., Berg, O. H., Hillamo, R., and Mäkela, T.: Chemical mass closure and assessment of the origin of the submicron aerosol in the marine boundary layer and the free troposphere at Tenerife during ACE-2, Tellus, 52B, 141–168, 2000.

Ruuskanen, T., Reisssell, A., Keronen, P., Aalto, P., Laakso, L., Grönholm, T., Hari, P., and Kulmala, M.: Atmospheric trace gas and aerosol particle concentration measurements in Eastern Lapland, Finland 1992–2001, Boreal Environ. Res., 8, 335–349, 2003.

Shantz, N. C., Aklilu, Y.-A., Ivanis, N., Leasitch, W. R., Brickell, P. C., Brook, J. R., Cheng, Y., Halpin, D., Li, S.-M., Tham, Y. A., Toom-Sauntry, D., Prenni, A. J., and Graham, L.: Chemical and physical observations of particulate matter at Golden Ears Provincial Park from anthropogenic and biogenic sources, Atmos. Enrivon., 38, 5849–5860, 2004.

Sofiev, M. P. and Siljamo, P.: Forward and inverse simulations with Finnish emergency model SILAM, in: Air Pollution Modelling and its Applications XVI, edited by: Borrego, C. and Incecik, S., Kluwer Acad./Plenum Publ., 417–425, 2003.

Spanke, J., Rannik, U., Forkel, R., Nigge, W., and Hoffmann, T.: Emission fluxes and atmospheric degradation of monoterpens above a boreal forest: field measurements and modelling, Tellus 53B, 406–422, 2001.

Wiedensohler, A., Covert, D. S., Swietlicki, E., Aalto, P., Heintzeberg, J., and Leck, C.: Occurrence of an ultrafine particle mode less than 20 nm in diameter in the marine boundary layer during Arctic summer and autumn, Tellus 48B, 213–222, 1996.